

Adaptive multirate time integration in the ARKODE library

Daniel R. Reynolds¹, Sylvia Amihere¹, Dashon Mitchell¹, Vu Thai Luan²

¹Department of Mathematics, Southern Methodist University

²Department of Mathematics, Texas Tech University

SIAM Conference on Computational Science and Engineering
Fort Worth, TX
5 March 2025

Outline

- 1 Multiphysics, Multirate Background
- 2 Time adaptivity
- 3 Results
- 4 Conclusions & future work

Outline

- 1 Multiphysics, Multirate Background
- 2 Time adaptivity
- 3 Results
- 4 Conclusions & future work

Multiphysics simulations [Keyes et al., 2013]

Multiphysics simulations couple together different physical models, either *in the bulk* or *across interfaces*.

Climate simulations are a good example:

- atmospheric simulations combine fluid dynamics with local “physics” models for chemistry, condensation, . . . , or
- atmosphere may be coupled at interfaces to myriad other processes (ocean, land/sea ice, . . .), each using distinct models.



[<https://e3sm.org>]

Multiphysics challenges [Keyes et al., 2013]

These combinations can challenge traditional numerical methods:

- “Multirate” processes evolve on different time scales but prohibit analytical reformulation.
- Stiff components disallow fully explicit methods.
- Nonlinearity and insufficient differentiability challenge fully implicit methods.
- Parallel scalability demands optimal algorithms – while robust/scalable algebraic solvers exist for parts (e.g., FMM for particles, multigrid for diffusion), none are optimal for the whole.

Implicit-explicit methods may be used to treat stiffness; here we focus on the multiple time scale issue. We consider a prototypical problem:

$$\dot{y}(t) = f^S(t, y) + f^F(t, y), \quad t \in [t_0, t_f], \quad y(t_0) = y_0.$$

- $f^S(t, y)$ contains the “slow” dynamics, naturally evolved with large steps H .
- $f^F(t, y)$ contains the “fast” dynamics, that evolves with small steps $h \ll H$.

Multirate Infinitesimal (MRI) methods

[Schlegel et al., 2009; Sandu, 2019; Fish, R., & Roberts, 2024]

MRI methods allow up to $\mathcal{O}(H^6)$ approaches to “subcycle” multirate problems. Denoting $y_n \approx y(t_n)$, a single explicit MRI step $t_n \rightarrow t_n + H$ proceeds as:

- ① Let: $Y_1 = y_n$
 - ② For $i = 2, \dots, s$:
 - ① Solve: $v_i'(\tau) = C_i f^F(\tau, v_i(\tau)) + r_i(\tau)$, for $\tau \in [\tau_{0,i}, \tau_{F,i}]$ with $v_i(\tau_{0,i}) = v_{0,i}$.
 - ② Let: $Y_i = v_i(\tau_{F,i})$.
 - ③ Solve: $\tilde{v}_s'(\tau) = C_s f^F(\tau, \tilde{v}_s(\tau)) + \tilde{r}_s(\tau)$, for $\tau \in [\tau_{0,s}, \tau_{F,s}]$ with $\tilde{v}_s(\tau_{0,s}) = v_{0,s}$.
 - ④ Let: $y_{n+1} = Y_s$ and $\tilde{y}_{n+1} = \tilde{v}_s(\tau_{F,s})$.
- MRI methods are uniquely defined by: leading constant C_i , fast stage time intervals $[\tau_{0,i}, \tau_{F,i}]$, initial conditions $v_{0,i}$, forcing functions $r_i(\tau)$, and embedding forcing function $\tilde{r}_s(\tau)$.
 - $r_i(\tau)$ and $\tilde{r}_s(\tau)$ are typically constructed using linear combinations of $\{f^S(\tau_{F,j}, Y_j)\}$, and propagate information from the slow to the fast time scale.
 - \tilde{y}_{n+1} is an embedded solution with a different order of accuracy than y_{n+1} .

Outline

- 1 Multiphysics, Multirate Background
- 2 Time adaptivity**
- 3 Results
- 4 Conclusions & future work

Single rate control

[Gustafsson, 1991; Söderlind, 2006]

- Traditional adaptivity controls *local error*, $e_n = y(t_n + H_n) - y_{n+1}$, assuming y_n is exact, adapting H_n to ensure $\varepsilon_n := \|e_n\| \leq 1$ where the norm incorporates the user tolerances, among other objectives.
- The controller \mathcal{C} typically depends on a few $(H_{n-k}, \varepsilon_{n-k})$ pairs, i.e.,

$$\tilde{H} = \mathcal{C}(H_n, \varepsilon_n, H_{n-1}, \varepsilon_{n-1}, \dots, p),$$

where p is the method order, i.e., $\varepsilon_n = c(t) H^{p+1}$, for some $c(t)$ independent of H .

- The simple *I controller* approximates c as piecewise constant, $c = \frac{\varepsilon_n}{h^{p+1}}$, to predict \tilde{H} :

$$1 = c\tilde{H}^{p+1} = \varepsilon_n \frac{\tilde{H}^{p+1}}{H^{p+1}} \quad \Leftrightarrow \quad \tilde{H} = \frac{H}{\varepsilon_n^{1/(p+1)}}.$$

- More advanced options exist, that typically use additional $(H_{n-k}, \varepsilon_{n-k})$ values to build higher-degree piecewise polynomial approximations of the principal error function.

For multirate control, we thus require both a strategy to estimate local temporal error ([Appendix](#)), and algorithms for selecting step sizes H and h .

MRI time step control – Decoupled (*Dec*) controllers

The simplest approach to MRI adaptivity is to use two decoupled single-rate controllers:

$$\begin{aligned}\tilde{H} &= \mathcal{C}^S(H_n, \varepsilon_n^S, H_{n-1}, \varepsilon_{n-1}^S, \dots, P), \\ \tilde{h} &= \mathcal{C}^F(h_{n,m}, \varepsilon_{n,m}^F, h_{n,m-1}, \varepsilon_{n,m-1}^F, \dots, p),\end{aligned}$$

where (H_k, ε_k^S) are the stepsize and local error estimates for time step k at the slow time scale, and $(h_{k,\ell}, \varepsilon_{k,\ell}^F)$ are the stepsize and local error estimates for the fast substep ℓ within the slow step k .

- \mathcal{C}^S and \mathcal{C}^F are independent of one another, so selection of \tilde{H} and \tilde{h} occurs independently.
- We expect this to work well for problems with weakly coupled time scales.
- Due to its decoupled nature, this trivially extends to an arbitrary number of time scales, allowing adaptivity for so-called “telescopic” MRI methods.

MRI time step control – Step-tolerance ($H\text{-}Tol$) controllers

For problems with more strongly coupled time scales, we may wish to request tighter accuracy from the inner solver. When called over fast intervals $[\tau_{0,i}, \tau_{F,i}]$, we assume the accumulated errors satisfy

$$\varepsilon_i^F = \chi(t) H_n \left(\text{reltol}_n^F \right),$$

where reltol_n^F is the relative tolerance requested of the inner solver, and $\chi(t)$ is independent of reltol_n^F .

This matches the single-rate controller assumption $\varepsilon_n = c(t)h^{p+1}$, where $\chi(t_n)H_n$ is $c(t)$, reltol_n^F is h , and $p = 0$. Thus any single-rate controller can adjust reltol_n^F between slow step attempts.

To construct an “ $H\text{-}Tol$ ” controller, we require three separate single-rate adaptivity controllers:

- $\mathcal{C}^{S,H}$ – single-rate controller to adapt H_n within the slow integrator.
- $\mathcal{C}^{S,Tol}$ – single-rate controller to adapt reltol_n^F above.
- \mathcal{C}^F – single rate controller to adapt $h_{n,m}$ within the fast integrator to achieve reltol_n^F .

This class of controllers also support telescopic multirate methods.

MRI time step control – Coupled ($H-h$) controllers

[Fish & R., SISC, 2023]

These extend the single-rate derivations [Gustafsson, 1994] by approximating both slow and fast principal error functions using piecewise polynomials. We proposed four multirate controllers that adapt H_n and $M_n = H_n/h_n$ (i.e., fast substeps are held constant over each slow step):

- *constant-constant*: $H_{n+1} = H_n (\varepsilon_{n+1}^S)^\alpha$, $M_{n+1} = M_n (\varepsilon_{n+1}^S)^{\beta_1} (\varepsilon_{n+1}^F)^{\beta_2}$,

- *linear-linear*: $H_{n+1} = H_n \left(\frac{H_n}{H_{n-1}} \right) (\varepsilon_{n+1}^S)^{\alpha_1} (\varepsilon_n^S)^{\alpha_2}$,

$$M_{n+1} = M_n \left(\frac{M_n}{M_{n-1}} \right) (\varepsilon_{n+1}^S)^{\beta_{11}} (\varepsilon_n^S)^{\beta_{12}} (\varepsilon_{n+1}^F)^{\beta_{21}} (\varepsilon_n^F)^{\beta_{22}}.$$

- *PIMR* (a multirate extension of the PI single-rate controller):

$$H_{n+1} = H_n (\varepsilon_{n+1}^S)^{\alpha_1} (\varepsilon_n^S)^{\alpha_2}, \quad M_{n+1} = M_n (\varepsilon_{n+1}^S)^{\beta_{11}} (\varepsilon_n^S)^{\beta_{12}} (\varepsilon_{n+1}^F)^{\beta_{21}} (\varepsilon_n^F)^{\beta_{22}}.$$

- *PIDMR* (a multirate extension of the PID single-rate controller):

$$H_{n+1} = H_n (\varepsilon_{n+1}^S)^{\alpha_1} (\varepsilon_n^S)^{\alpha_2} (\varepsilon_{n-1}^S)^{\alpha_3},$$

$$M_{n+1} = M_n (\varepsilon_{n+1}^S)^{\beta_{11}} (\varepsilon_n^S)^{\beta_{12}} (\varepsilon_{n-1}^S)^{\beta_{13}} (\varepsilon_{n+1}^F)^{\beta_{21}} (\varepsilon_n^F)^{\beta_{22}} (\varepsilon_{n-1}^F)^{\beta_{23}}.$$

Outline

- 1 Multiphysics, Multirate Background
- 2 Time adaptivity
- 3 Results**
- 4 Conclusions & future work

Kværno-Prothero-Robinson (KPR) test problem

$$\begin{pmatrix} u'(t) \\ v'(t) \end{pmatrix} = \begin{bmatrix} G & e \\ e & -1 \end{bmatrix} \begin{pmatrix} (u^2 - p - 2)/(2u) \\ (v^2 - q - 2)/(2v) \end{pmatrix} + \begin{pmatrix} p'(t)/(2u) \\ q'(t)/(2v) \end{pmatrix}, \quad 0 \leq t \leq 5,$$

where $p(t) = \cos(t)$ and $q(t) = \cos(\omega t(1 + e^{-(t-2)^2}))$.

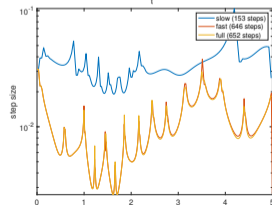
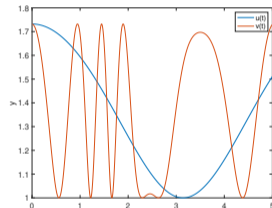
The analytical solution is $u(t) = \sqrt{2 + p(t)}$ and $v(t) = \sqrt{2 + q(t)}$.

Here:

- e that determines the strength of coupling between the time scales,
- $G < 0$ determines the stiffness at slow time scale,
- w that determines the time-scale separation factor.

At right: analytical solutions with parameters $G = -10$, $e = 1/10$, $\omega = 5$.

Top: solutions. Bottom: internal single-rate time steps.



Embedded MRI methods

We test MRI adaptivity using embedded MRI methods:

- MRI-GARK methods from [Sandu, 2019]:
 - Explicit MRI_ERK22a, MRI_ERK22b, MRI_ERK33a, and MRI_ERK45a methods (orders 2, 2, 3, 4);
 - Implicit MRI_IRK21a, MRI_ESDIRK34a, and MRI_ESDIRK46a methods (orders 2, 3, 4);
- the explicit, $\mathcal{O}(H^2)$ MRI_RALSTON2 MRI-GARK method from [Roberts, 2022];
- IMEX-MRI-SR methods of order 2, 3, and 4 from [Fish, R., & Roberts, 2024]: MRISR21, MRISR32, and MRISR43;
- explicit MERK methods of orders 2, 3, 4, and 5 from [Luan, Chinomona, & R., 2020] with custom embeddings: MERK21, MERK32, MERK43, and MERK54.

Each of the above methods include an embedding with order of accuracy one lower.

MRI adaptive method accuracy

Detailed results regarding the accuracy obtained by each controller type and MRI method are provided in the [Appendix](#), where we compare the ability of each MRI method and controller to achieve the

target accuracy over all components l and time steps n :
$$\text{accuracy} = \max_{n,l} \left| \frac{y_{n,l} - y_{ref,l}(t_n)}{\text{abstol} + \text{reltol} |y_{ref,l}(t_n)|} \right|.$$

- Multirate factors $\omega = \{5, 50, 250, 500\}$:
 - Both *Dec* and *H-Tol* achieve accuracy ratios $\lesssim 10$ for all ω .
 - *H-h* had accuracy $\lesssim 10$ for $\omega = 5$ and $\text{reltol} = 10^{-3}$, but struggled as ω increased.
- reltol ranging from 10^{-3} down to 10^{-7} :
 - *Dec* and *H-Tol* controllers also achieve solutions within $\sim 10x$ of the target across all reltol .
 - *H-h* accuracy ratios deteriorated as tolerances were tightened.
- Low-order vs high-order MRI methods:
 - All controllers improved when using higher-order MRI methods.
 - *H-Tol* had $\sim 20\%$ better accuracy than *Dec*, which was $\gtrsim 100x$ better than *H-h*.
 - Most MRI methods performed similarly at each order, but there were outliers.

MRI adaptive method cost

Detailed results regarding cost of each method shown above are provided in the [Appendix](#). Highlights:

- Number of slow time steps [assumed to be expensive]:
 - *H-Tol* controllers are $\sim 10\%$ better efficiency than *Dec*.
 - Both *H-Tol* and *Dec* are $\sim 10x$ more efficient than *H-h*.
- Number of fast time steps [assumed to be inexpensive]:
 - *H-h* controllers are $\sim 3x$ lower cost than *Dec* and *H-Tol*.
 - *Dec* controllers are $\sim 10\%$ lower cost than *H-Tol*.
- Number of rejected slow time steps:
 - Both *H-Tol* and *Dec* reject a very small fraction of slow steps, with *H-Tol* rejecting $\sim 20\%$ fewer than *Dec*.
 - *H-h* reject $\sim 10x$ more steps than both *H-Tol* and *Dec* (up to $\sim 20\%$).

Outline

- 1 Multiphysics, Multirate Background
- 2 Time adaptivity
- 3 Results
- 4 Conclusions & future work**

Conclusions and future work

Conclusions:

- Both the *Dec* and *H-Tol* families show robust adaptive control across a wide range of: multirate ratios ($\omega = 250$ and 500 ; 5 and 50 were similar), relative tolerances (10^{-7} up to 10^{-3}), and low and high order embedded MRI methods.
- Of the two, *H-Tol* had slightly better accuracy and computational efficiency.
- However, *H-h* struggled to meet accuracy, and had significantly higher “slow” cost. This indicates it may artificially constrain the step size ratio $M_n = H_n/h_n$.

Note: all of these results were performed using the ARKODE solver from the SUNDIALS library. Its newest release (Dec. 2024) includes both Dec and H-Tol controller families.

We are currently extending these results to additional multirate applications:

- We have similar results for a stiff Brusselator test (will be included in forthcoming paper).
- Large-scale application codes, including *Perturbo* (solid state physics) and *BOUT++* (fusion).

Thank you for your time and attention!

- For more information on any of our new methods research, please see my webpage: <https://people.smu.edu/dreynolds>.
- For more information on SUNDIALS, please see our
 - project page on Github: <https://github.com/llnl/sundials>
 - documentation: <https://sundials.readthedocs.io>
- For anything else, send me an email: reynolds@smu.edu
- I will soon be advertising to hire a postdoc – if you are interested, please let me know!

This work was supported by the U.S. Department of Energy, Office of Science, Office of Advanced Scientific Computing Research (ASCR) via the Frameworks, Algorithms, and Software Technologies for Mathematics Institute Scientific Discovery through Advanced Computing (SciDAC) program.

5 Appendix

MRI temporal error estimation – ε_n^S and ε_n^F

Slow error may be estimated as usual for embedded methods, $\varepsilon_n^S = \|y_n - \tilde{y}_n\|$, but non-intrusive estimates for ε^F are more challenging. We consider four strategies:

- Three assume that at each sub-step $t_{n,m}$ the fast integrator computes a local error estimate, $\varepsilon_{n,m}^F$, and itself is temporally adaptive with relative tolerance, reitol^F . We accumulate these via:

$$\varepsilon_{n,max}^F = \text{reitol}^F \max_{m \in M} \varepsilon_{n,m}^F \quad \text{“Maximum accumulation,”}$$

$$\varepsilon_{n,add}^F = \text{reitol}^F \sum_{m \in M} \varepsilon_{n,m}^F \quad \text{“Additive accumulation,” or}$$

$$\varepsilon_{n,avg}^F = \varepsilon_{n,add}^F / |M| \quad \text{“Average accumulation,”}$$

where M is the set of all steps since the fast error accumulator has been reset.

- The fourth uses fixed fast steps h and kh to compute y_h^F and y_{kh}^F , estimating

$$\varepsilon_{n,dbl}^F = \frac{\|y_h^F - y_{kh}^F\|}{|k^p - 1|} \quad \text{“Double-step accumulation,”}$$

where p is the global order of accuracy for the fast method.

Accumulated error comparisons

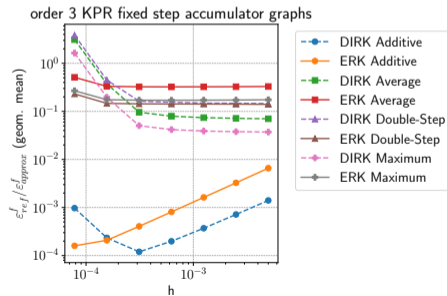
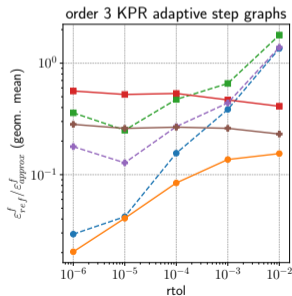
We partition the integration interval into subintervals, $t_0 < t_1 < \dots < t_{20} = t_f$, and evolve over each $[t_k, t_{k+1}]$, with the initial condition reset to the reference solution $y_{ref}(t_k)$. We compare the estimates ε_X^F against the “true” value of the fast error, $\varepsilon_{ref}^F(t_{k+1})$ via the ratio

$$\text{ratio}_X(t_{k+1}) = \frac{\varepsilon_{ref}^F(t_{k+1})}{\varepsilon_X^F(t_{k+1})},$$

Left: adaptive fast integration.

Right: fixed-step fast integration.

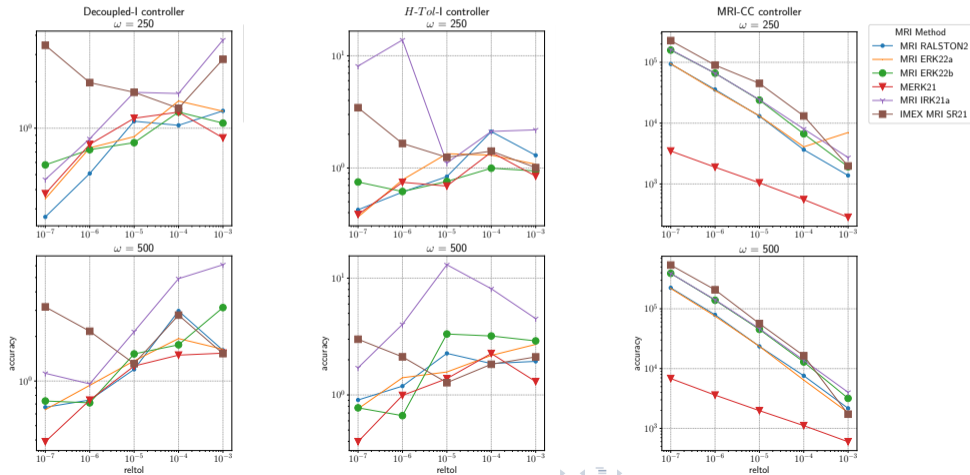
All except Additive report accumulated error within $\sim 10\times$ of actual across tolerances/steps.



MRI adaptive accuracy – second-order methods

We compare the ability of each MRI method and controller to achieve the target accuracy over all

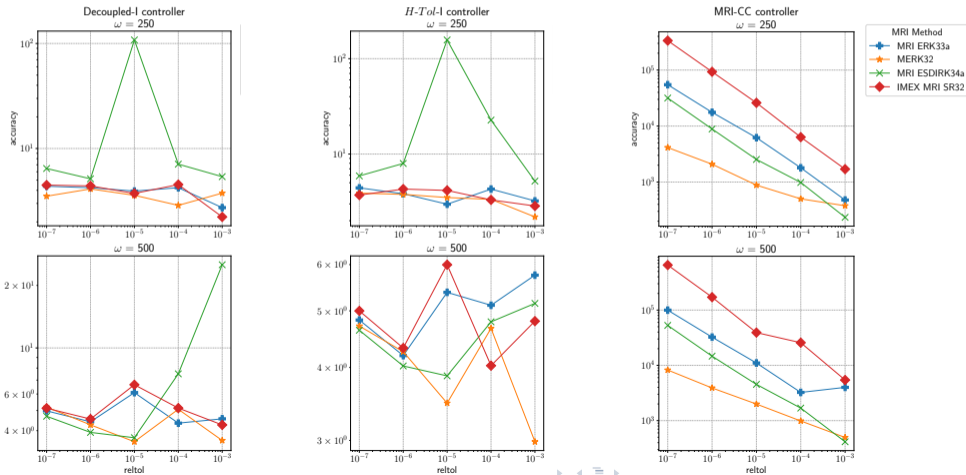
components l and time steps n :
$$\text{accuracy} = \max_{n,l} \left| \frac{y_{n,l} - y_{ref,l}(t_n)}{\text{abstol} + \text{reltol} |y_{ref,l}(t_n)|} \right|.$$



MRI adaptive accuracy – third-order methods

We compare the ability of each MRI method and controller to achieve the target accuracy over all

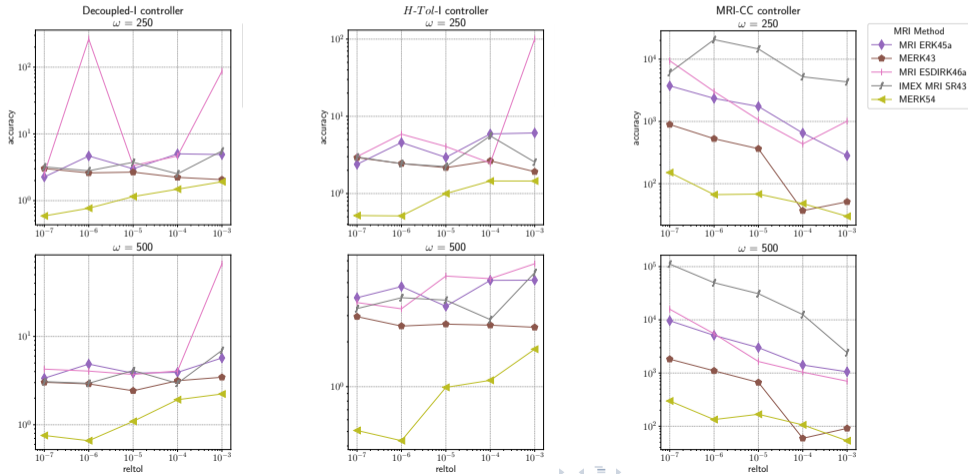
components l and time steps n :
$$\text{accuracy} = \max_{n,l} \left| \frac{y_{n,l} - y_{ref,l}(t_n)}{\text{abstol} + \text{reitol} |y_{ref,l}(t_n)|} \right|.$$



MRI adaptive accuracy – higher-order methods

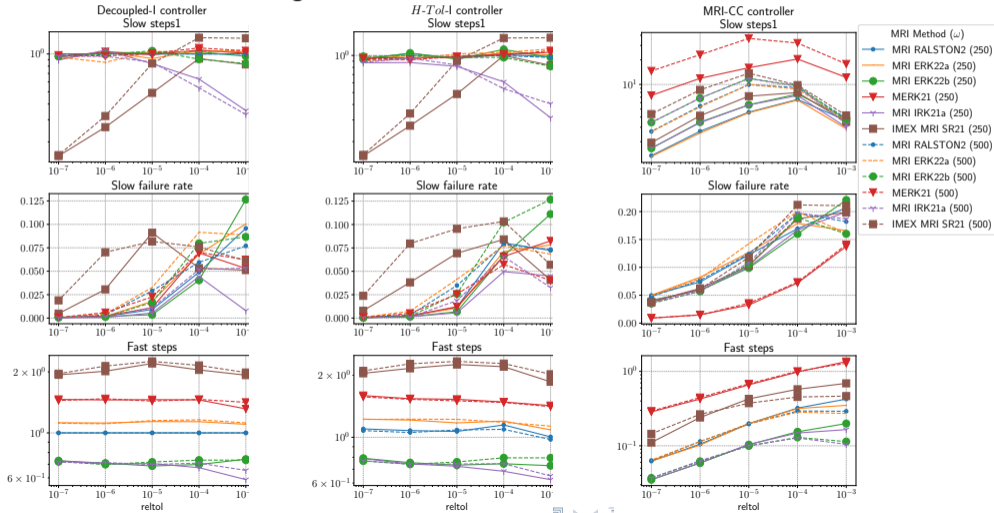
We compare the ability of each MRI method and controller to achieve the target accuracy over all

components l and time steps n :
$$\text{accuracy} = \max_{n,l} \left| \frac{y_{n,l} - y_{ref,l}(t_n)}{\text{abstol} + \text{reltol} |y_{ref,l}(t_n)|} \right|.$$



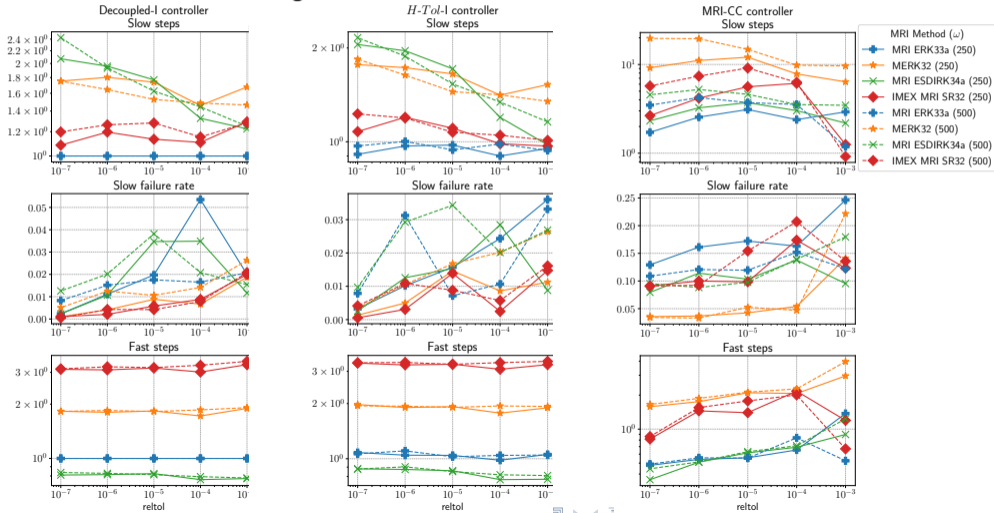
MRI adaptive cost – second-order methods

We compare the numbers of slow and fast steps (normalized to MRI_RALSTON2 with *Dec-I* controller), and slow failure rate across a range of tolerances.



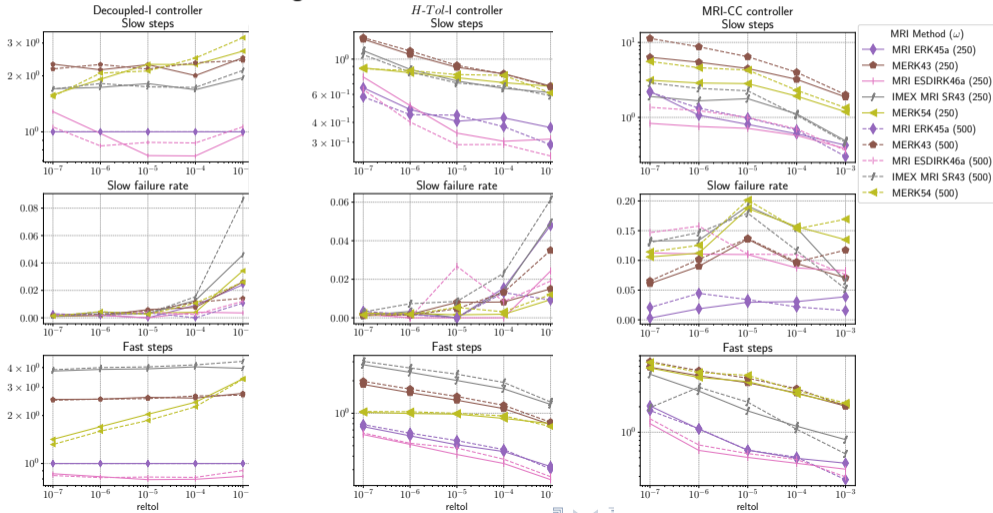
MRI adaptive cost – third-order methods

We compare the numbers of slow and fast steps (normalized to MRI_ERK33a with *Dec-I* controller), and slow failure rate across a range of tolerances.



MRI adaptive cost – higher-order methods

We compare the numbers of slow and fast steps (normalized to MRI_ERK45a with *Dec-I* controller), and slow failure rate across a range of tolerances.



MRI adaptive step histories

We plot the slow and fast step size histories for a few adaptivity controller types at $\text{reltol} = 10^{-5}$, listing the total numbers of slow and fast time steps, and ability to achieve the target accuracy.

